fibers

MDPI

Article

Synthesis of Lignin/PAN Fibers from Sawdust

Meruyert Nazhipkyzy [1,2,*], Anar B. Maltay [1,2], Bakhytzhan Lesbayev [1,2] and Dana D. Assylkhanova [2]

[1] Department of Chemical Physics and Material Science, Al-Farabi Kazakh National University, Almaty 050040, Kazakhstan
[2] Institute of Combustion Problems, Almaty 050012, Kazakhstan; dana.asylkhanova16@gmail.com
* Correspondence: meruert82@mail.ru

Abstract: Carbon nanofibers based on lignin from wood waste have a promising potential for the ability to produce electrodes that can modernize existing energy storage technology. The most important detail is that the low cost, as well as the availability of the initial products for the production of lignin, will reduce the cost of energy storage devices and contribute to improving the environment. In this study, pine sawdust and elm sawdust were used as raw materials for the production of lignin, which accumulate in large quantities in metal workshops in Almaty. Lignin extraction was carried out using an organosolvent method, which is environmentally friendly, low-cost, uses minimal amounts of strong acids and metal catalysts, does not pollute water, and does not emit sulfur dioxide (SO_2). A comprehensive study of the characteristics of the obtained lignins from wood waste was carried out. Infrared spectroscopy (IR) revealed that the obtained lignin contains aromatic, phenolic, hydroxyl, methyl, and methoxyl groups. The results of nuclear magnetic resonance (NMR) spectroscopy showed the presence of a high number of syringyl (S) links compared to guaiacyl (G), which contribute to increased efficiency in the thermal processing of lignin. Also, this study investigated the use of the obtained lignins to produce continuous fibers by electrospinning. The effect of lignin mass on the viscosity of the lignin/polyacrylonitrile (PAN) solution and the effect of the carbonization temperature on the physico-chemical characteristics of the lignin/PAN solution were investigated. The following research methods were used for this purpose: Raman spectroscopy, thermogravimetric analysis (TGA), electron scanning microscopy, energy dispersion analysis, IR, NMR, and optical microscopy. The conditions for the production of lignin-containing carbon fibers at temperatures of 800, 900, and the carbonation heating rate, is an important parameter in the production of carbon fibers as it strongly affects the characteristics of the resulting carbon fibers. The heating rate affects were studied, and it was found that, at a heating rate of 5 °C/min and a carbonation temperature of 800 °C, porous carbon nanofibers with a diameter of 47 nm are formed in a nitrogen medium for 60 min.

Keywords: lignin/PAN fibers; electrospinning; anode; supercapacitors; Li-ion batteries

Citation: Nazhipkyzy, M.; Maltay, A.B.; Lesbayev, B.; Assylkhanova, D.D. Synthesis of Lignin/PAN Fibers from Sawdust. *Fibers* **2024**, *12*, 27. https://doi.org/10.3390/fib12030027

Academic Editor: Umesh Prasad Agarwal

Received: 7 December 2023
Revised: 17 January 2024
Accepted: 27 January 2024
Published: 13 March 2024

1. Introduction

Today, the use of energy in the form of fossil fuels causes catastrophic damage to the ecology of our planet; therefore, the growing demand for energy requires the development of sustainable, renewable, and environmentally friendly energy sources [1,2]. Wood as a raw material is widely used in many industries. Its processing leads to the accumulation of huge amounts of waste in the form of sawdust and non-condensing lumber; therefore, the problem of recycling wood waste is urgent [3]. Although waste recycling methods, such as the production of wood slabs, pellets, and fuel briquettes, are well mastered, due to a number of technological limitations and the requirement of additional costs, a huge part of wood waste remains unused. Non-recyclable wood waste is mainly incinerated or disposed of in landfills; in both these cases, greenhouse gases are emitted and the environment is polluted simultaneously.

Today, plants are the most common source of biomass in the field of bioenergy. Biomass is an extremely complex matrix containing chemical components in various ratios, including cellulose, hemicellulose, and lignin, as well as small amounts of protein, fat, ash, and phenolic compounds [4–6]. Recent research has focused on the use of inexpensive sawdust as an energy source. Lignin is a complex, three-dimensional, aromatic biopolymer, which is the second most widespread biofield in the world, and the second most frequently used renewable natural resource, after cellulose [7]. According to the latest data, the accumulation of lignin in the world annually amounts to about 60 million tons, which is environmentally hazardous. The amount of this lignin used each year is on average 5%. Therefore, the utilization of lignin is an important problem today. According to a recent research report, the combined annual growth rate of the lignin market (CAGR) is 2.2% [8]. There are several methods for extracting lignin from biomass: alkali treatment [9], oxidation [10], organosolvent processes [11], biological purification [12], etc. There are known works describing the production of pure lignin by the organosolvent method, in which a mixture of organic solvents are used. According to one study [13], the presence of a catalyst in the reaction can increase the purity of lignin. Among acid catalysts, the use of formic acid is relevant since it has a high ability to dissolve lignin at low temperature and pressure [14]. In [7], the use of mineral acids, such as sulfuric acid and hydrochloric acid, in the synthesis of lignin is considered. It should also be noted that the softening temperature for lignin ranges from 160 to 190 °C [15], and this leads to self-melting during heating and carbonation of the lignin fiber. According to Fodil Ch. and others [16], the physicochemical properties and thermal stability of the organosolvent method and kraft lignin from the biomass of deciduous and coniferous rocks were compared. The authors found that lignin extracted from hardwood using the kraft process has the highest yield. In [17], optimal conditions for lignin extraction with maximum yield from wheat straw by the organosolvent method were established. Thus, the characteristics and properties of lignin depend on the chemical composition, the origin of the initial product, and the extraction method. Currently, three main methods of obtaining polymer fibers are used: stretching, template synthesis, and electroforming via electrospinning. Among these methods, nanoscale fibers can only be obtained using electrospinning since nanofibers of polymers that can withstand large deformations while in a viscous state can be obtained by stretching, and long nanofibers cannot be obtained using the template method. After the publication of the work by Lallav M. et al. [18] on the use of electricity for the manufacture of carbon fibers based on lignin, the number of studies related to the conversion of lignin into carbon nano-fibers is steadily growing. Lignin has a relatively low molecular weight, depending on its plant source and extraction method. In most cases, when lignin is electroformed, droplets are formed from the spray instead of fibers. Therefore, electrospinning requires the presence of another polymer with a higher molecular weight. Polyacrylonitrile (PAN), polyvinyl alcohol (PVA), or polyethylene glycol (PEG) are usually used. PAN is very common as a binder polymer for the manufacture of carbon nanofibers (CNF) based on lignin due to its easy formability, high molecular weight, and the possibility of conversion into carbon fibers with relatively high mechanical strength [19–22]. The disadvantages of PAN are that it is expensive, and its disposal requires additional material costs. In recent years, active efforts have been made to develop lignin as an active precursor for the production of carbon fiber [23]. In [24], a decrease in fiber diameter was observed as the carbonation temperature increased. The diameter of lignin fibers is also important for the mechanical properties of carbonized fibers. Reducing the diameters of lignin fibers can improve the mechanical properties of lignin-based carbon fibers to a certain extent [25]. Currently, fibrous composite materials made of lignin are used in new non-structural products, such as energy storage devices, for example, batteries [26,27] and capacitors [28–31]. In this work, experimental studies were conducted on the construction of electrodes based on carbon nanomaterials for supercapacitors. Lignin-based carbon nanofibers from wood waste have a promising potential for producing electrodes capable of modernizing existing energy storage technologies. The most important detail is that the low cost, as well as the

availability of initial products for the production of lignin, will reduce the cost of energy storage devices and contribute to environmental improvement.

2. Materials and Methods

Pine sawdust and elm sawdust, which accumulate in large quantities in the furniture workshops of Almaty, were used as raw materials for the production of lignin. To obtain the lignin-containing fibers, the following materials were used: polyacrylonitrile (PAN) ((-CH_2-CH-(CH)-)$_n$, molecular weight: 100,000 g/mol, St. Louis, MO, USA) and dimethylformamide (DMF) ((CH_3)$_2$NC(O)H, Sigma Aldrich (St. Louis, MO, USA), 99.8%).

To study the surface morphological features of lignin and lignin/PAN fibers, scanning electron microscopy (SEM) ("Quanta 200i 3D", FEI company, Hillsboro, OR, USA) was used in the open-type nanotechnology laboratory at the Al-Farabi Kazakh National University. The functional properties and purity of the obtained lignin were studied using non-destructive IR spectroscopy. The samples were analyzed using an IR spectrometer, Spectrum 65 model, Perkin Elmer, Waltham, MA, USA, in the wavelength range of 450 to 4000 cm^{-1} with a resolution of 4 cm^{-1}. To study the phase composition of the sample, studies were carried out using Raman spectroscopy. This method determines the degree of graphitization and the ordering of the carbon structure. The degree of graphitization was calculated using Formula (1):

$$G_f = \frac{A(G)}{\sum_{500}^{2000} A} \times 100\% \quad (1)$$

where: G_f is the degree of graphitization;

$A(G)$—peak G area;

$\sum A$—full spectrum region.

The degree of graphitization calculated from the spectra increases with increasing carbonation temperature. These carbon-containing materials with partial graphitization are very suitable for use as electrodes due to their high electronic conductivity.

The surfaces and morphological features of the obtained lignin/PAN fibers were analyzed using SEM (SEM, JEOL, model JSM-6490LA). Analysis was performed on a Solaar Spectrum (NT-MDT) Raman spectrometer (wavelength 473 nm, signal accumulation time 30 s). The thermal stability and decomposition of organic polymers were investigated via thermogravimetric analysis (TGA). The TGA results were obtained in a nitrogen atmosphere at temperatures ranging from room temperature to 1000 °C at a heating rate of 20 °C/min. ^{1}H NMR spectra were taken on a JNM-ECA Jeol400 spectrometer (frequency 399.78 MHz) using DMSO-d_6 solvent.

2.1. Obtaining Lignin from Wood Waste Using the Organosolvent Method

The organosolvent method, which was was the main process used to obtain lignin in this study, is shown in Figure 1. In total, 8.5 g of sawdust was placed in a vessel, a solution of formic and acetic acid with a volume ratio of 70:30 was added (Figure 1(1,2)), and the resulting mixture was treated with constant stirring for 2.5 h at a temperature of up to 115 °C. The first signs of the decomposition reaction were observed after only 5 min of heating the solution. In the first stage, there was an intense change in the color of the solution, ranging from light brown to dark red (Figure 1(3)). As the reaction developed, the color became darker and wood clusters also dispersed. Then, the mixture was cooled to 25 °C, and undissolved impurities were filtered out. Water was added to the resulting concentrated extract at a ratio of 5:1. The mixture was heated to a temperature of 105 °C, and lignin precipitation was carried out. After adding water to the mixture, the color changed to light orange, and the formation of larger lignin agglomerates was observed (Figure 1(4)).

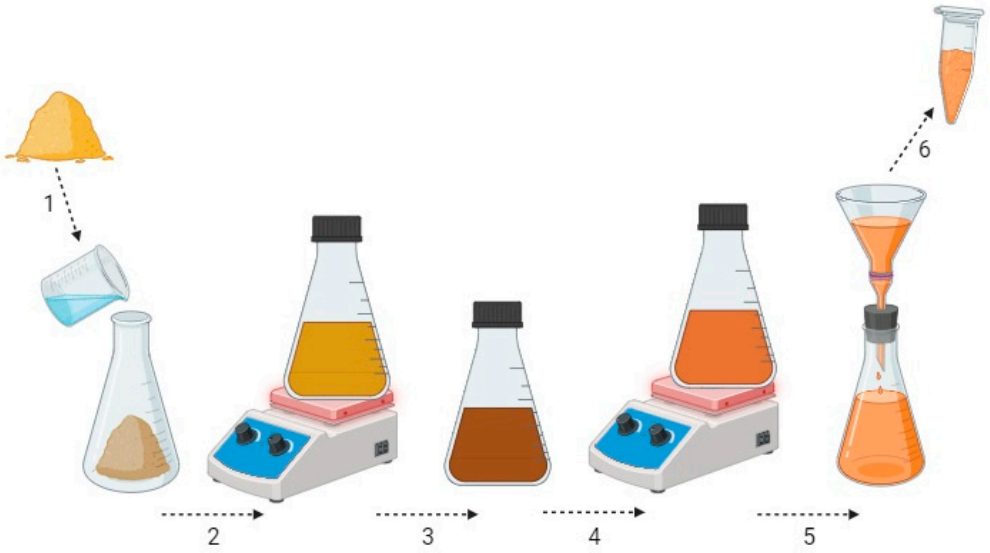

Figure 1. The process of obtaining lignin from wood waste: (1) sawdust; (2) type of solution immediately after adding sawdust; (3) type of solution after 1 h; (4) type of solution after adding water; (5) filtration; (6) lignin.

After 30 min, lignin was deposited in the form of agglomerates. After cooling the resulting mixture to room temperature, the formed lignin was separated using a centrifuge (5 min, 5000 rpm). The isolated lignin precipitate was washed with distilled water until a neutral pH was reached, dried for 24 h at ambient temperature, and then additionally dried in a vacuum drying cabinet for 1 h at a temperature of 60 °C (Figure 1(5)). Lignin obtained via this method does not contain carbohydrates or sulfur, which is very important for the further processing of lignin into carbon fibers (Figure 1(6)). Using the method described above, three types of lignin were obtained: lignin from mixed wood waste (MWW) with a yield of 19.3%, elm sawdust with a yield of 18%, and pine sawdust with a yield of 16.7%. The obtained lignin powders were characterized using SEM, IR spectroscopy, TGA, and NMR.

2.2. Obtaining Fibers from Lignin/PAN via Electrospinning

Figure 2 shows a general schematic representation of an installation for producing fibers via electrospinning. The synthesis of fibers from the obtained spinning solutions was carried out on a NanoFiber desktop electric spinning system for laboratory research from AME Energy, Shenzhen, China (model number: AME-11, power: 220 V, 50/60 Hz). The parameters of the fiber synthesis process varied within the following limits: the operating voltage was 13 kV, the flow rate of the supplied spinning solution varied from 0.4 mL/h to 0.8 mL/h, and the distance between the needle and the substrate varied from 100 to 180 mm. The formed fibers were deposited on a substrate representing a rotating drum. The spinning solution for pulling lignin-containing fibers via electrospinning included three components: PAN, lignin, and a DMF solvent. Various amounts of lignin were added to the PAN solutions to obtain solutions containing 0, 10, 20, 30, 40, 50, 60, 70, 80, 90, and 100% lignin (in relation to the mass of the PAN). The solutions were prepared by mixing them at room temperature with constant stirring until the components were completely dissolved.

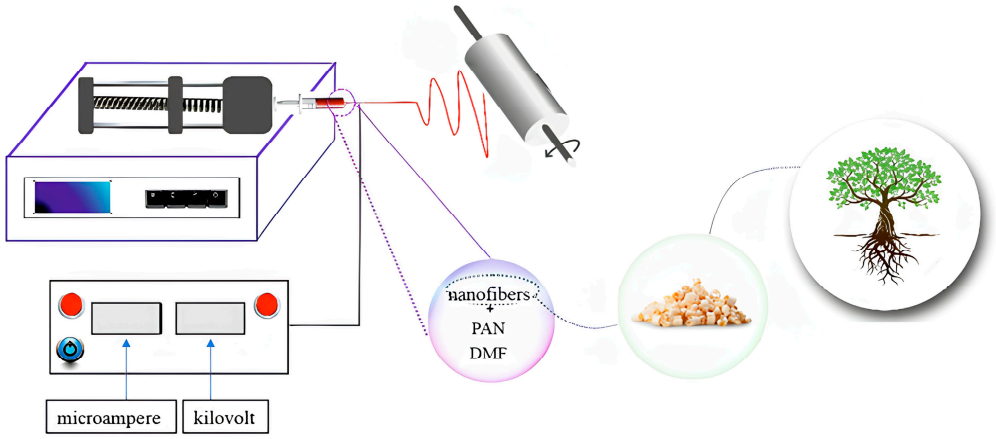

Figure 2. Diagram of the experimental installation for electrospinning.

2.3. Stabilization and Carbonation of the Obtained Fibers

Lignin/PAN fibers were transformed into carbon fibers via thermal stabilization (in air) followed by carbonization (in nitrogen). These processes were carried out in a tubular furnace with three 1600 °C temperature zones (model PT-T1600-L6012CB3, Zhengzhou Protech Technology Co., Ltd., Zhengzhou, China). The accuracy/temperature control range was ±1 °C, and the recommended heating speed was 0–10 °C/min, with a maximum of 20 °C/min. At a heating rate of 5 °C/min, the sample was maintained for 1 h when the temperature reached 800, 900, and 1000 °C. The carbonization process of the obtained fibers was carried out in a nitrogen medium. The nitrogen consumption was 120 mL/min. During the carbonization process, dehydration and decarboxylation occurred, carbon atoms were crosslinked, aromatization reactions occurred, and most of the non-carbon elements were released. Photos of the fibers after the thermal stabilization and carbonization processes are shown in Figure 3.

Figure 3. Photos of fibers after thermal stabilization processes and carbonization: (1) fibers from 30/70 lignin/PAN on the substrate; (2,3) the type of fibers removed from the substrate; (4) fibers after the thermal stabilization process; (5) fibers after the carbonization process.

The structural characteristics and morphology of the carbon fibers were studied using SEM, TGA, elemental analysis, and Raman spectroscopy.

2.4. Manufacturing of Electrodes Based on Carbon Nanofibers for Supercapacitors

The manufacture of a current collector, in which the obtained carbon fibers were protected on both sides by a metal substrate, consisted of the following stages. The first stage was the creation of a rough surface on the initial metal surface that could provide high adhesion. To obtain the substrate, stainless steel foil was used (the thickness of the foil was 0.4 mm; SS 316L grade). The thickness and uniformity of the foil, as well as the foil coated with carbon material, was controlled by a thickness gauge equipped with micrometers. To obtain a rough surface, the metal foil was pre-processed on both sides mechanically. A mechanical treatment with sandpaper (with a grain size of P1000 and GOI paste no. 3) on the substrate surface created greater roughness on the surface than chemical etching, which

ensured good adhesion of the porous layer to the current collector and electrical contact. Also, the mechanical surface treatment is an environmentally friendly method since acids are not used in the process. The polished foil was cut into several samples of rectangular current collectors.

The second stage was the process of degreasing the treated substrate by placing it in an ultrasonic bath, first in ethanol and then in distilled water, followed by drying in a drying cabinet at a temperature of 120 °C for 2 h.

The third stage was the process of applying a layer of suspension, with a thickness of ≈400 microns and an area of 1 × 2 cm^2, to a pre-prepared metal foil using laboratory spatulas. The pre-prepared suspension consisted of carbon fiber and a plasticizer. The optimal ratio for the electrode material components was 70% carbon nanofibers, 15% acetylene soot to increase electrical conductivity, and 15% PVDF binder polymer. The process of making the suspension was carried out in an agate mortar with intensive stirring for 5 min, and the solvent 1-methyl-2-pyrrolidone was added in the form of drops until a homogeneous viscous mixture was obtained.

The fourth and final stage included a heat treatment of the applied suspension layer in a vacuum drying cabinet for 12 h at a temperature of 120 °C.

3. Results and Discussion

3.1. Physical and Chemical Characteristics of Lignins Obtained from Wood Waste

Figure 4 shows SEM micrographs of lignin obtained via the organosolvent method in which the prevalence of macropores can be observed. In a sample of lignin from elm sawdust (c), the pores ranged up to approximately 100 microns; in a sample of lignin from pine sawdust (b), the pores were over 100 microns; and in a sample of lignin from MWW (a), the pores were about 100 microns. An important characteristic of lignin is the presence of the functional groups included in the lignin structure, which were determined using the non-destructive IR spectroscopy method. The results from MWW, pine sawdust, and elm sawdust are shown in Figure 5. The vibrational spectra obtained in certain regions indicate the presence of functional groups corresponding to the lignin in the molecules.

Figure 6 shows the IR spectra of the obtained lignins, which indicate the presence of functional groups that are characteristic of coniferous wood and the purity of the obtained lignins. It is known that the lignins of coniferous wood contain more carbon–carbon bonds and fewer ether bonds than the lignins of deciduous wood. This means that hardwood lignin has a more compact structure than softwood lignin. The main difference between the lignins of deciduous and coniferous species is in the functional groups. In the IR spectrum of lignin, there are absorption bands at 3435 cm^{-1}, belonging to hydroxyl groups in phenolic and aliphatic structures, and 2926 cm^{-1} bands, resulting from the stretching of CH in aromatic methoxyl and methyl groups. Since aliphatic groups form intermolecular hydrogen bonds, it is expected that coniferous lignin has a larger network of hydrogen bonds than hardwood lignin. Coniferous lignin has a higher OH band, which corresponds to a more rigid structure and implies a higher glass transition temperature for coniferous lignin. The bands in the regions of 1603 and 1512 cm^{-1} correspond to aromatic compounds (phenolic hydroxyl groups) resulting from skeletal vibrations of aromatic rings in lignin. These bands are used to determine the type of lignin and the content of lignin in softwood fibers. The lignin content in softwood fibers is determined with high accuracy by measuring the intensity of the C=C vibrational bands of the aromatic ring bonds at 1512 cm^{-1}. The spectra of all the lignins show a band that is characteristic of the syringyl (S) ring plus the guaiacyl (G) ring in the condensed state. Vibrational bands at 1375 cm^{-1} (syringil) and 1270 cm^{-1} (guaiacil) indicate the presence of both syringil and guaiacil in the chemical structure of lignin [32]. These units form the basic building blocks that make up lignin from any source. It is also important to note that G units facilitate crosslinking. This affects the reactivity and thermal stability of lignin with a large number of G-links [33]. Based on the results of the spectrogram, we can say that the extracted product was lignin and did not contain other organic inclusions.

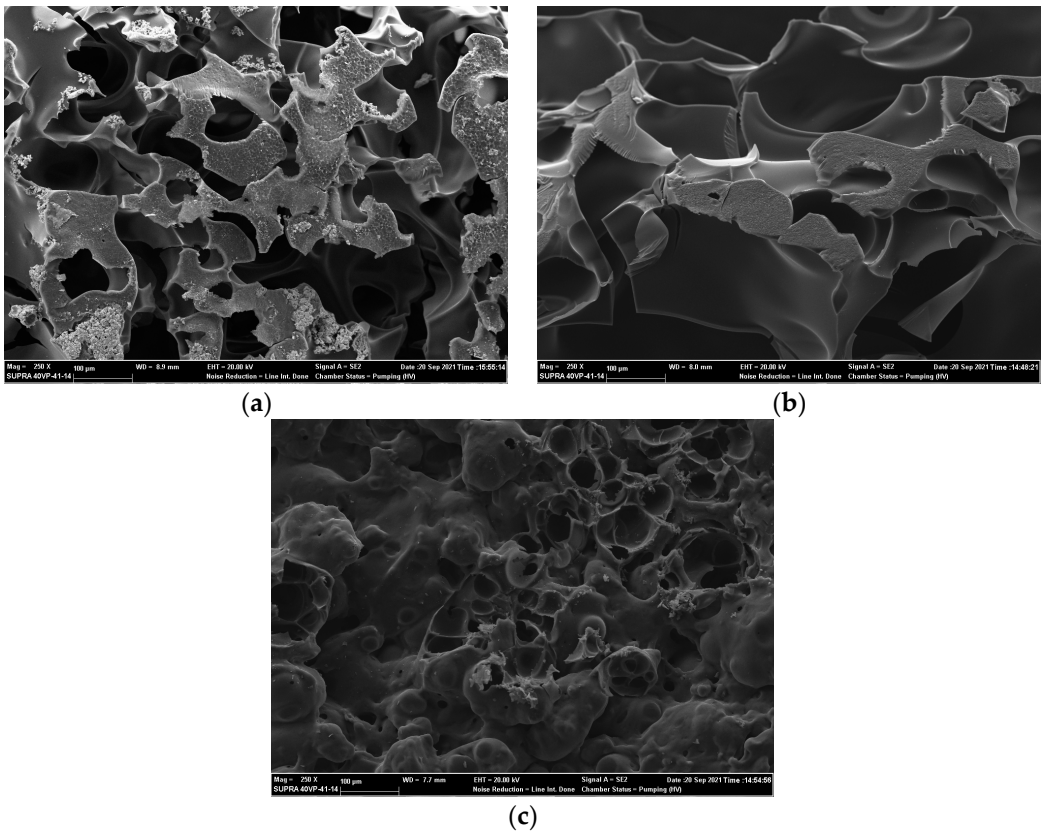

Figure 4. SEM images of the obtained lignins: (**a**) lignin from MWW; (**b**) pine lignin; (**c**) lignin from elm.

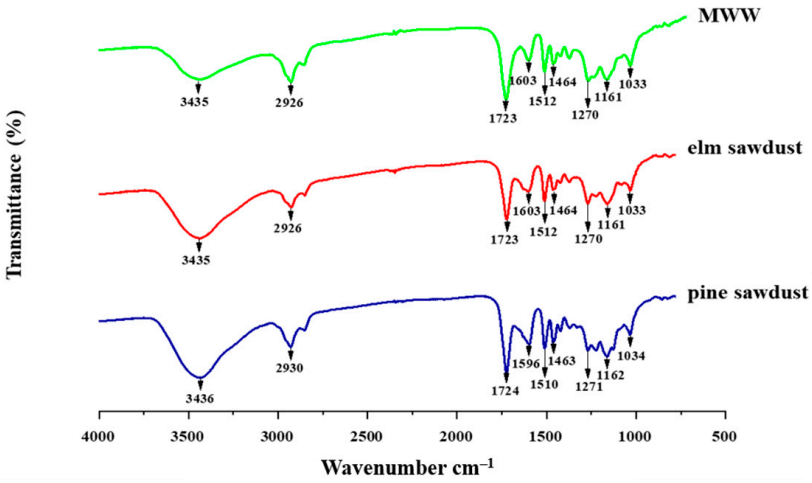

Figure 5. IR spectra of the obtained lignins.

Table 1 shows the characteristic bands of the infrared spectra of the obtained lignins.

The structural components of lignin and related hydroxyl groups were studied using the NMR method, and the obtained NMR spectra of the lignins are shown in Figure 6. The characteristic attributions of the received signals and the chemical shifts in the ^{1}H NMR spectrum of lignins are shown in Table 2.

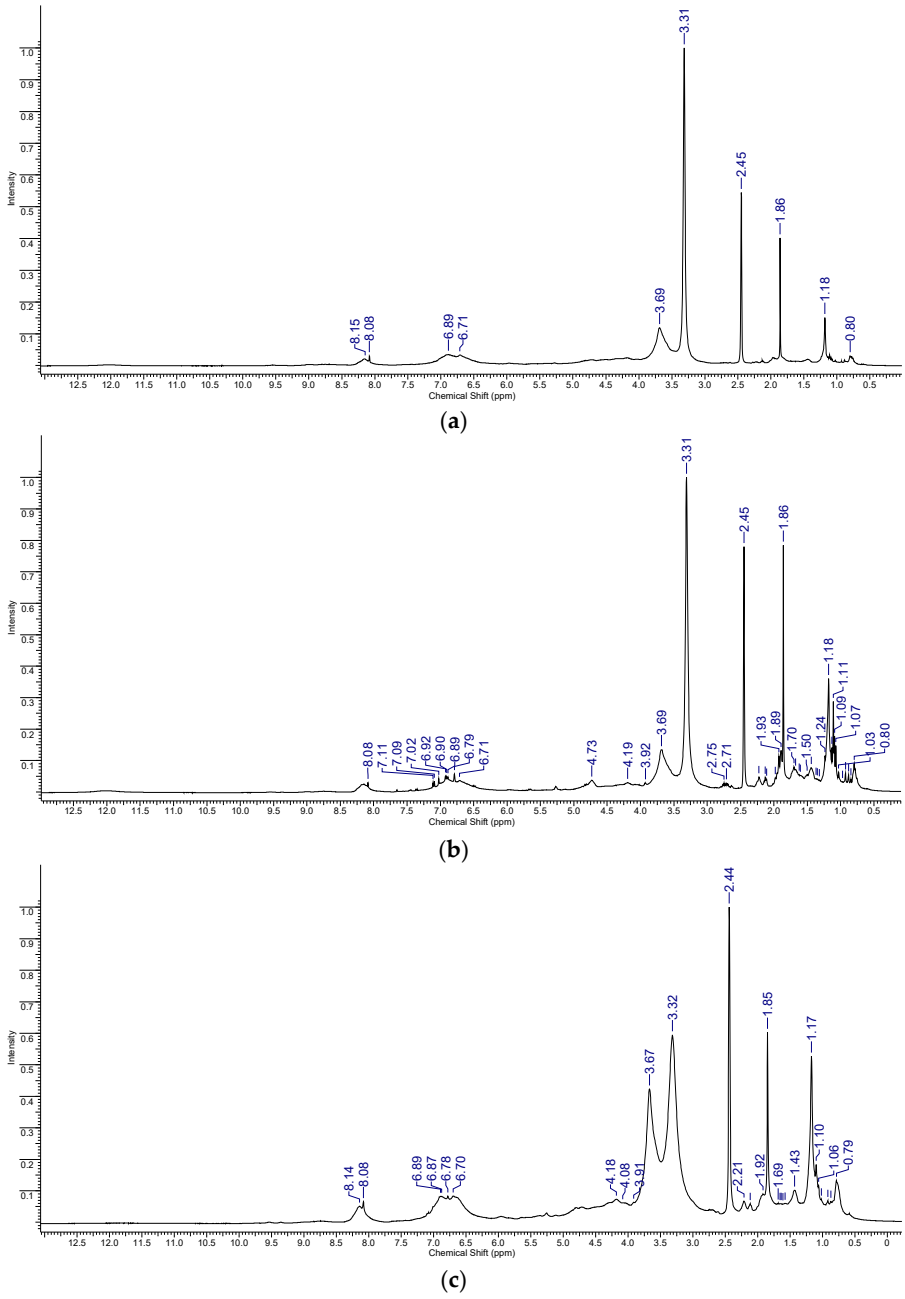

Figure 6. NMR spectra of the obtained lignins: (**a**) lignin from MWW; (**b**) pine lignin; (**c**) lignin from elm.

According to the NMR results shown in Figure 6, the lignin spectra show the appearance of signals in the region of 6.7 ppm, which characterize the presence of aromatic protons in the structures of syringylpropane and guaiacylpropane fragments of lignin [34]. The intensity of the proton signals in the region of 6.7–6.8 ppm indicates a higher content of syringyl (S) links compared to guaiacyl (G) in the studied lignin [35]. An increase in the number of S units present in the lignin structure improves the thermal processing of lignin. The presence of the phenolic hydroxyls of syringil was determined by the presence of chemical shifts at 8.08–8.15 ppm in the three studied samples of lignin [36]. The fractions of phenolic hydroxyl groups are directly responsible for the thermal mobility of lignin. The presence of phenolic hydroxyl contributes to the fusibility of lignin. This is because intramolecular hydrogen bonds can form between neighboring phenolic hydroxyl units, as well as between phenolic hydroxyl units and methoxyl groups. However, it is noted that

aliphatic hydroxyl units have a higher tendency to form hydrogen bonds than phenolic hydroxyl units do. Intense signals in the spectrum in the range of 3.32–3.67 ppm confirm the presence of methoxyl (-OCH_3) and methylenoxy- (-CH_2O-) fragments, which play an important role in the pyrolysis of lignin. Methoxyl groups prevent crosslinking and increase the free volume by inhibiting chain entanglement, which leads to higher chain mobility. The spectra show the appearance of signals at chemical shifts of 2.45–4.73 ppm, which correspond to two aromatic protons in the structures of syringyl and guaiacylpropane. The signals at 0.80 and 1.2 ppm refer to methyl and methylene protons in saturated aliphatic lignin side chains. Stronger intermolecular hydrogen bonds are formed between aliphatic hydroxyl groups, which leads to higher glass transition temperatures and affects the fusibility of lignin. The strength of the hydrogen bonds in lignin depends on the number of aliphatic hydroxyl groups, which depends on the cleavage reactions during the extraction and processing of the fibers.

Table 1. Characteristic bands of the IR spectrum of lignin.

Wave Number (cm^{-1})	Functional Group
3435	O–H (phenolic), hydrogen bonding
2926	C–H (alkane) in methyl groups
1723	C=O (non-conjugated carbonyl/carboxyl sprains)
1603	C=C (aromatic)
1512	C=C (aromatic)
1464	C–H (deformation, asymmetric)
1270	C–O (ether)
1161	C–H (aromatic) with flat deformation
1033	C–O (ether)

Table 2. Characteristic signal assignment and chemical shifts in the ^1H NMR spectra of the extracted lignins.

Chemical Shift (ppm)	Appointment
0.80–1.2	Methyl and methylene protons
2.21	Aromatic acetate
2.45–4.73	Signals in this region refer to two aromatic protons in the structures of syringil and guaiacylpropane
6.70–7.11	Aromatic protons

Based on the above findings, it can be concluded that making significant progress in the work of lignin-derived carbon fibers depends on a very clear understanding of the structure, chemical composition, and changes in the structure of lignin as it is being processed into final products. According to the results of studies conducted using the methods of IR spectroscopy, SEM, and NMR, lignins obtained from elm sawdust, pine sawdust, and mixed sawdust are almost the same. In this regard, sawdust from mixed waste has been selected for the production of fibers since the disposal of mixed waste is a more urgent issue. This is because different types of sawdust are formed during woodworking operations from various tree species in large quantities, which harms the environment. During production, sawdust is not sorted by the type of tree, it is simply collected in one pile as waste and occupies a huge area. In developing countries, the accumulation of wood waste from different types of trees is increasing every year; for example, 40% of waste remains during sawmilling. As there is a lack of space for wood waste disposal, from an ecological point of view, the damage to the environment is recognized as an urgent issue, and the wood waste requires processing or disposal.

3.2. Physical and Chemical Characteristics of Carbon Nanofibers Based on Lignin/PAN

The surface, structure, and morphology of the obtained lignin/PAN fibers were analyzed using optical (Figure 7a) and scanning microscopes (Figure 7b).

As a result of comparing the optical images shown in Figure 7a, we can say that lignin/PAN fibers are an example of a one-dimensional nanomaterial in the form of long continuous homogeneous nanofibers.

The conducted studies have shown that, when using a spinning solution of 8 wt.%, continuous nanoscale fibers are formed from a mixture of lignin and PAN for electrospinning (Figure 7b). According to the SEM images, the diameters of the obtained continuous lignin/PAN fibers are 7 wt.% from 125 to 440 nm, 8 wt.% from 88 to 123 nm, and 9 wt.% from 215 to 440 nm. It should be noted that, with a decrease in the diameter of the obtained fibers, their functional and mechanical properties increase. This is because, when the diameter of the electro-spun polymer nanofiber is less than the threshold value, its tensile strength and axial modulus increase dramatically [37,38]. In the course of the conducted studies, it was found that the optimal condition for the formation of continuous nanofibers is a concentration of 8 wt.%. The effect of the lignin mass on the viscosity of the lignin/PAN solution was recorded at lignin contents of 0, 10, 20, 30, 40, 50, 60, 70, 80, 90, and 100 wt.% (relative to the mass of the pan). The structural properties of the obtained lignin/PAN mixtures of various compositions were determined using the SEM method (Quanta 200i 3D) to determine the morphology of the electroformed fibers containing different lignin concentrations (Figure 8). The resulting SEM images were further studied, and ImageJ 1.54e software was used to measure the fiber diameter.

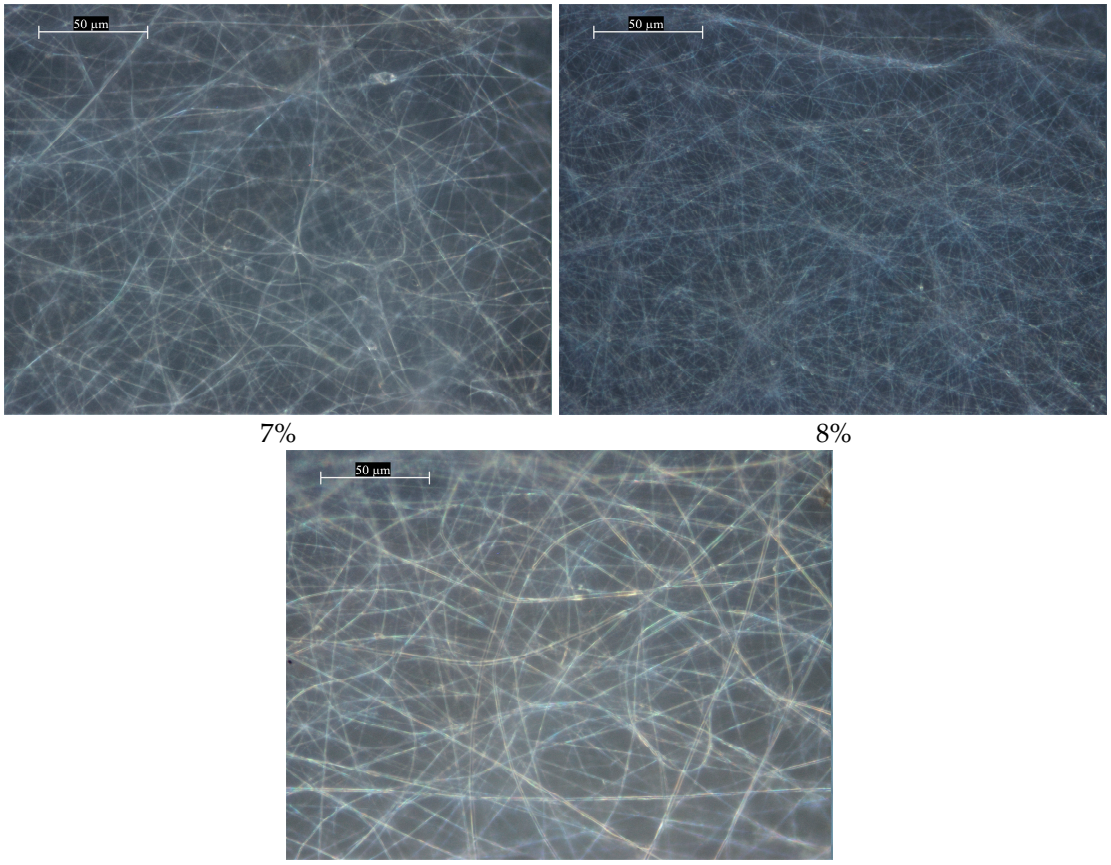

Figure 7. *Cont.*

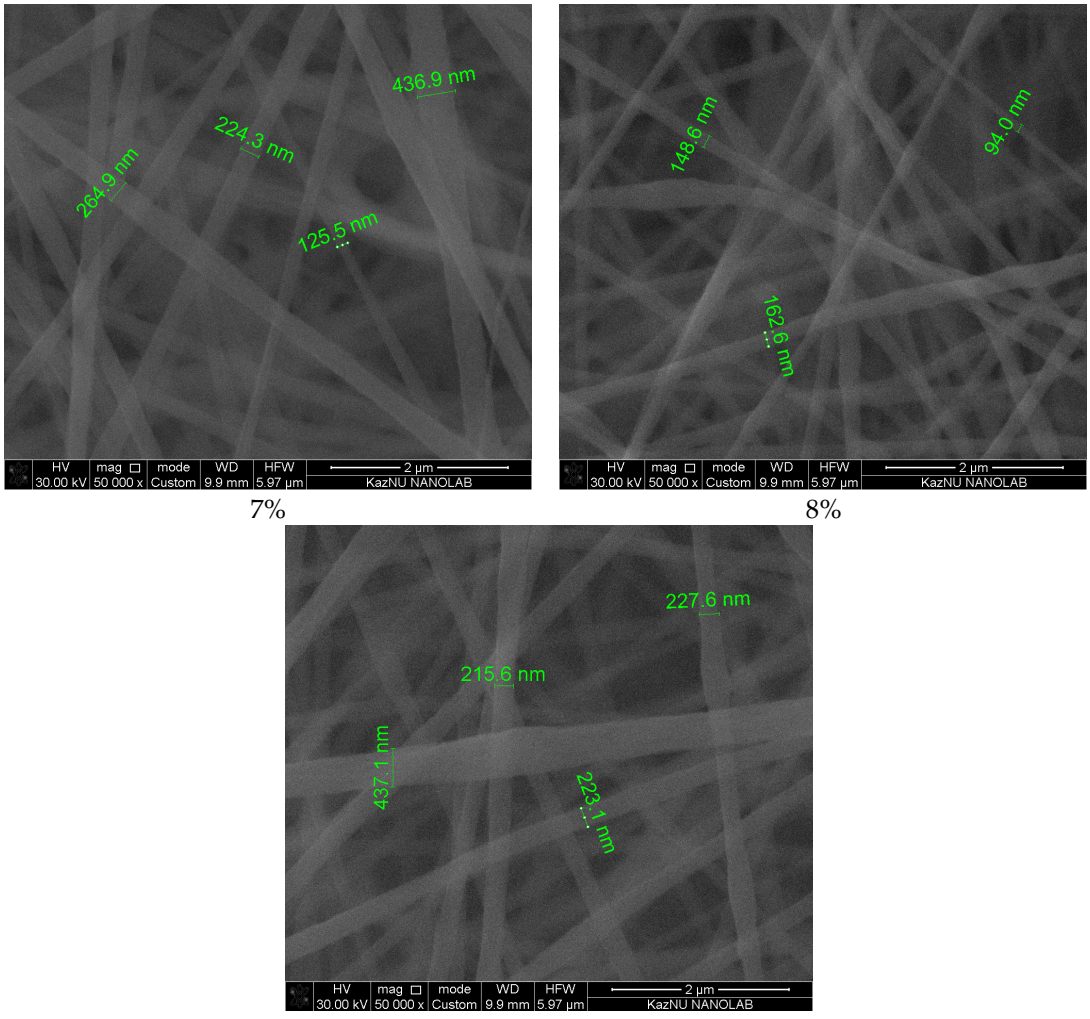

7% 8%

9%

(**b**)

Figure 7. Optical and SEM images of lignin/PAN fibers: (**a**) optical images; (**b**) SEM images.

We studied the effect of the percentages of lignin and PAN on the process of fiber formation via electrospinning. The fibers obtained from lignin/PAN at ratios of 10/90, 20/80, and 30/70 demonstrated a smooth and defect-free surface morphology with fiber diameters over 90 nm. With lignin/PAN ratios of 40/60 and 50/50, fibers with diameters of 70 nm or more were obtained; however, in the obtained samples, the formation of a small number of defects in the form of balls was observed. And at lignin/PAN ratios of 60/40, 70/30, and 80/20, the formation of defects in the form of beads was observed in the fibers. We associate the formation of beads with the process of forming the "ball on a string" structure described in the literature, which is an unfavorable phenomenon that occurs during electrospinning when the surface tension of the spinning solution prevails over the effects of electrostatic repulsion and the viscoelastic force, i.e., two inter-related factors that regulate the formation of fibers during electrospinning [39]. At a higher lignin/PAN ratio of 90/10, the formation of microspheres and microparticles of lignin was observed. It is worth noting that, for a spinning solution with PAN, the surface tension varies moderately depending on the polymer concentration, while the viscosity and conductivity of a solution can vary significantly to influence the formation of beads in electroformed fibers. When fibers are obtained from lignin without the addition of PAN, inhomogeneous interconnected balls are produced in the form of microspheres and microparticles of lignin with a diameter of 122 nm. Low-molecular-weight lignin cannot form an effective chain entanglement, which gives it a tendency to rupture during the formation of the fiber.

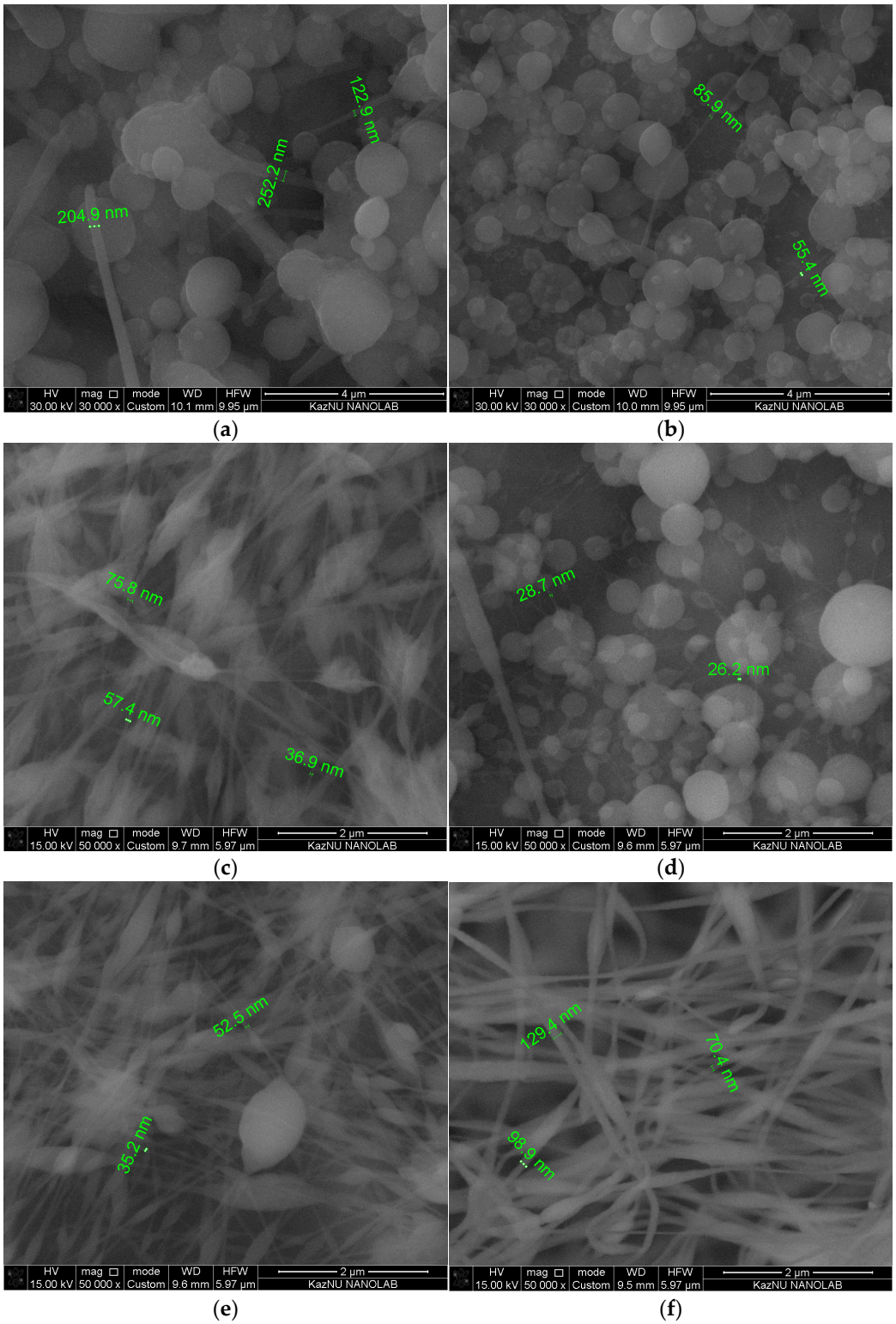

Figure 8. *Cont*.

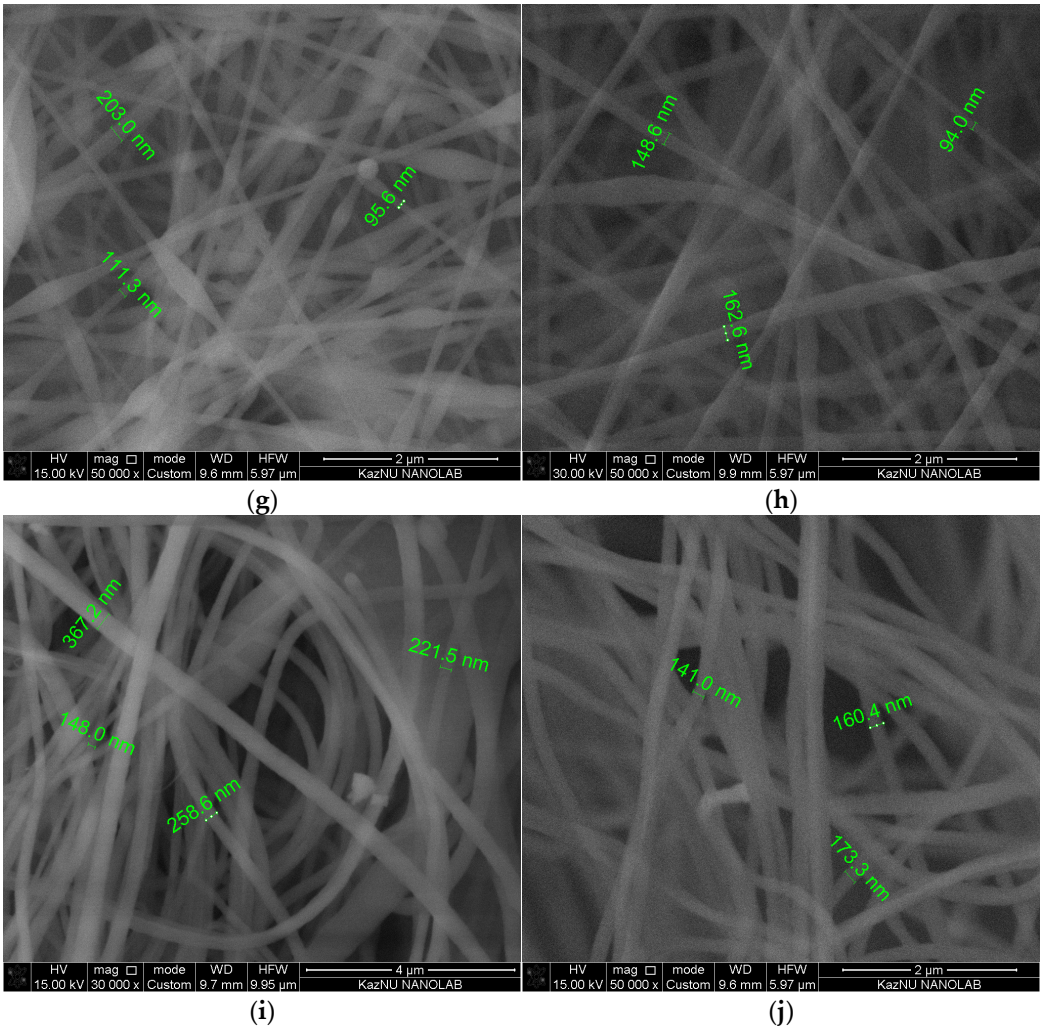

Figure 8. SEM images of lignin/PAN fibers: (**a**) pure lignin; (**b**) 90/10 lignin/PAN; (**c**) 80/20 lignin/PAN; (**d**) 70/30 lignin/PAN; (**e**) I 60/40 lignin/PAN; (**f**) 50/50 lignin; (**g**) 40/60 lignin/PAN; (**h**) 30/70 lignin/PAN; (**i**) 20/80 lignin/PAN; (**j**) 10/90 lignin/PAN.

Thus, for electric spinning, the solution must have a minimum concentration of lignin, below which bead fibers are formed. An increase in the content of PAN reduces the formation of defects in the form of balls but, at the same time, leads to an increase in the diameter of the fibers. Based on the data described above, it was found that the optimal percentage ratios of lignin and PAN for the formation of continuous nanoscale fibers without defects were 30/70.

SEM micrographs of carbon fibers from 30/70 lignin/PAN shown in Figure 9.

According to the SEM micrographs, the diameters of the continuous lignin/PAN fibers before carbonization were over 88 nm. After carbonization, there was a noticeable decrease in the diameters of the obtained continuous carbon fibers: over 47 nm at a carbonization temperature of 800 °C (Figure 9a); over 130 nm at 900 °C (Figure 9b); and over 75 nm at 1000 °C (Figure 9c). In the process of carbonization, non-carbon atoms leave the material in the form of volatiles and evaporation. During this process, the content of methoxy and carbonyl carbon atoms decreases, and the proportion of aryl and condensed aryl carbon atoms increases. According to the SEM micrographs presented in Figure 9, changes in the structure of the obtained fibers are observed in the form of defects with an increase in the carbonization temperature. This is due to the formation of aryl structures at low carbonization temperatures of 800 °C, and it is assumed that carbonization at high temperatures of 900–1000 °C leads to the destruction of some aryl structures formed at

lower temperatures (800 °C). It is expected that the breaking of aryl ether bonds will lead to a decrease in the number of aliphatic hydroxyl groups and an increase in phenolic hydroxyl units. A decrease in the number of aliphatic hydroxyl units leads to a decrease in the strength of hydrogen bonds and, consequently, to high thermal mobility. The presence of a higher concentration of aryl ether bonds increases the thermal mobility of lignin and reduces the glass transition temperature.

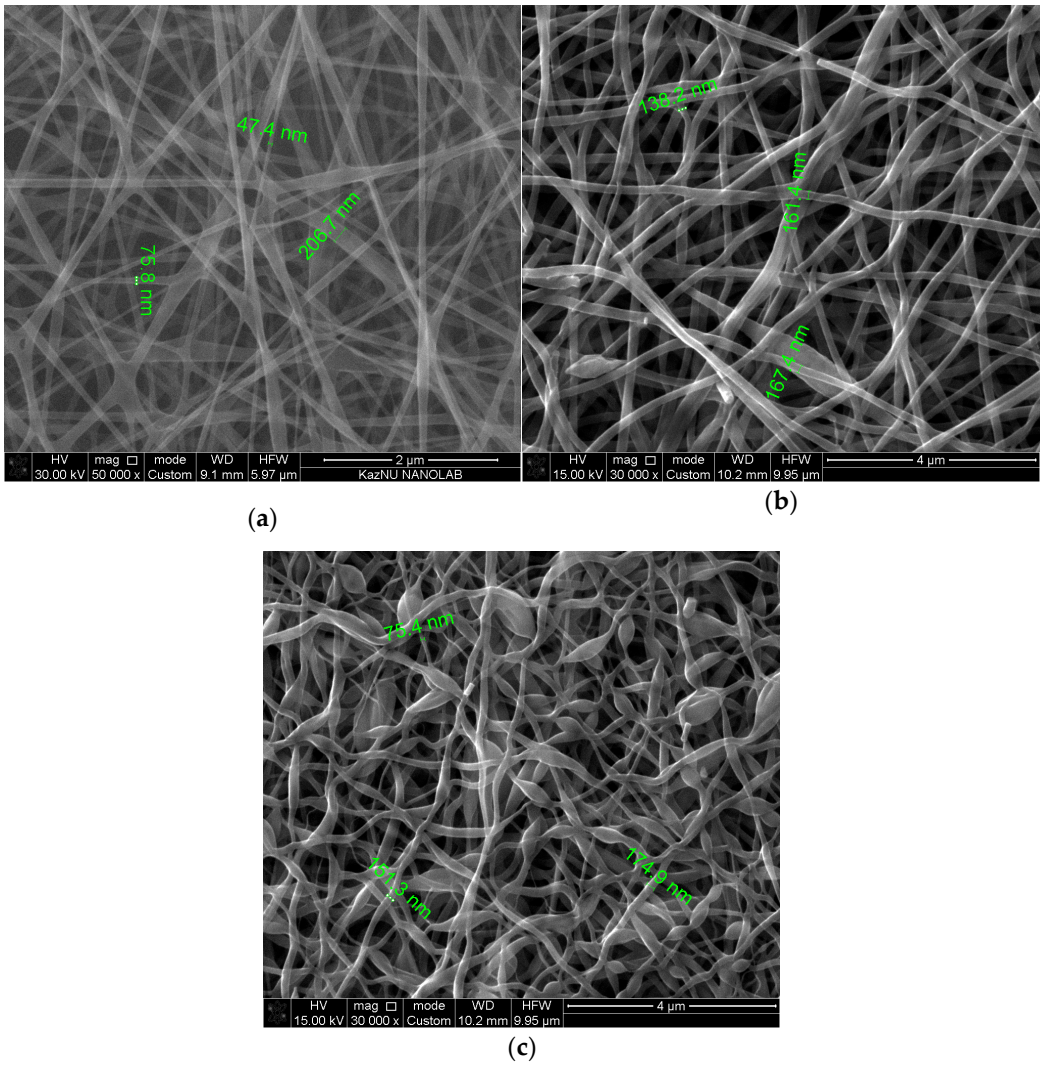

Figure 9. SEM micrographs of carbon fibers from 30/70 lignin/PAN carbonized at temperatures of: (**a**) 800 °C; (**b**) 900 °C; (**c**) 1000 °C.

The thermogravimetric analysis (TGA) was used to study the changes in the mass of the obtained nanofibers. For more information, a graph of the dependence of the weight loss on temperature was also plotted. This graph is called the DSC curve and can be used to determine the maximum temperature of each decomposition product. It is very useful in the characterization of lignin since it can be used to indicate the temperature at which a component of the lignin/PAN fiber decomposes. The TGA results of the obtained fibers are shown in Figure 10.

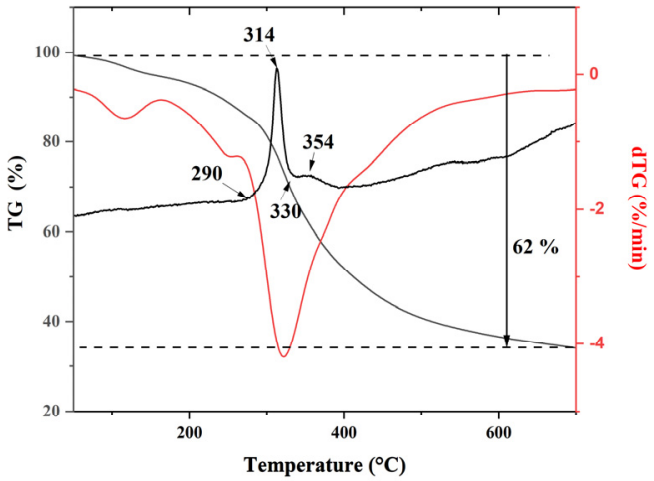

Figure 10. Thermogravimetric (TG) and derivative thermal analysis (DTG) curves for lignin/PAN 30/70 nanofibers.

The TG curves show that the decomposition of PAN begins at 290 °C, and the decomposition of lignin begins at 330 °C (Figure 10). The decrease in fiber weight below 100 °C is explained by the loss of adsorbed water. The presence of water can cause the connection of individual lignin molecules through hydrogen bonds. It also leads to the formation of a semi-coke when processing lignin at high temperatures as water acts as a reducing agent in such conditions. In the temperature range from 100 to 500 °C, lignin/PAN fibers showed a two-stage degradation due to differences in the thermal stability of their oxygen-containing functional groups. The presence of low-temperature volatile substances reduces the temperature of thermal decomposition, which leads to the formation of pores. Volatile substances in lignin/PAN fibers can occur due to carbohydrate impurities and the aliphatic hydroxyl link, which release water and formaldehyde at relatively low temperatures, as well as phenols with lower molecular weights. The presence of a large number of hydroxyl groups can also lead to lower thermal decomposition since they are prone to water absorption and lose water at low temperatures during heat treatment. As the TG curves show, the percentage of mass loss of lignin/PAN fibers relative to the temperature of thermal decomposition is 62%, and the yield of semi-coke is 38%. Lignin-based carbon fibers from coniferous wood have a relatively high carbon yield compared to other woods [40,41].

The diameters of the nanofibers in a set of SEM images were determined using the ImageJ software. The distribution of the diameters of the electrically spun fibers is shown in Figure 11. According to the histogram, the calculated average diameter of the fibers obtained from the solution of lignin/PAN at a ratio of 30/70 is in the range between 90 and 128 nm, with an average fiber diameter of 97 nm. To build a histogram of the fiber size distribution, 100 points were determined.

The structural characteristics of the carbon fibers were determined using X-ray diffraction (XRD) with Cu Kα radiation (λ = 1.54 Å) (Bruker). The X-ray diffraction patterns analysis of the carbon fibers are shown in Figure 12.

To determine the compositions of the crystalline and amorphous states of the carbon nanofibers, they were examined using X-ray diffraction analysis (Figure 12). The X-ray diffraction analysis of the CNF illustrates the presence of two characteristic wide carbon peaks, including diffraction from the {002} planes located at an angle of 24.7°, which indicates a disordered carbon structure [42], and diffraction from the {100} planes at an angle of 43.6°, corresponding to the turbostrate carbon plane [43]. The wide peak shape of about 24.1° indicates that carbon nanofibers are mainly composed of amorphous carbon. The average distance between layers {002} and {100} was calculated using the Bragg equation (Table 3).

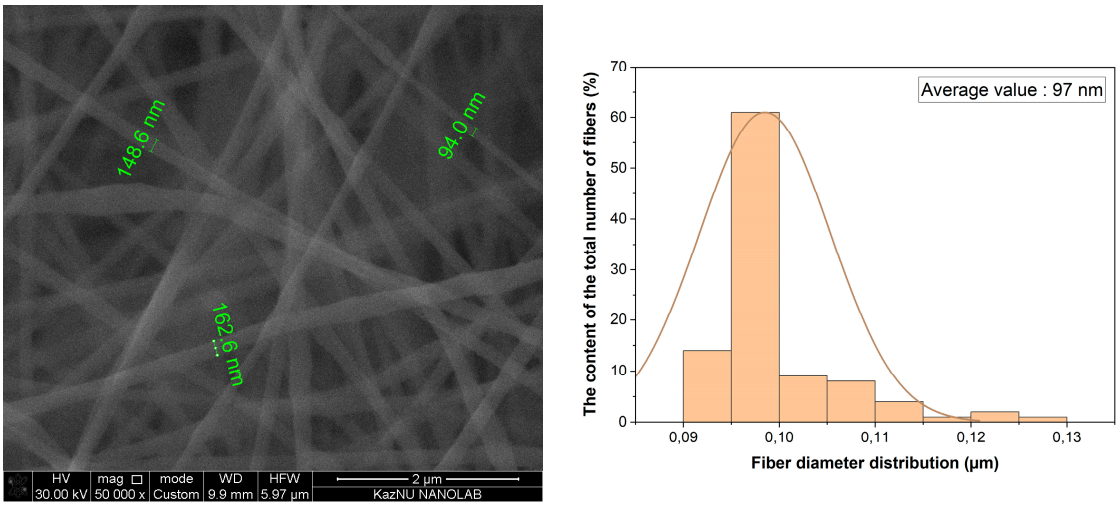

Figure 11. SEM micrography (**a**) of lignin/PAN fiber with fiber size distribution (**b**).

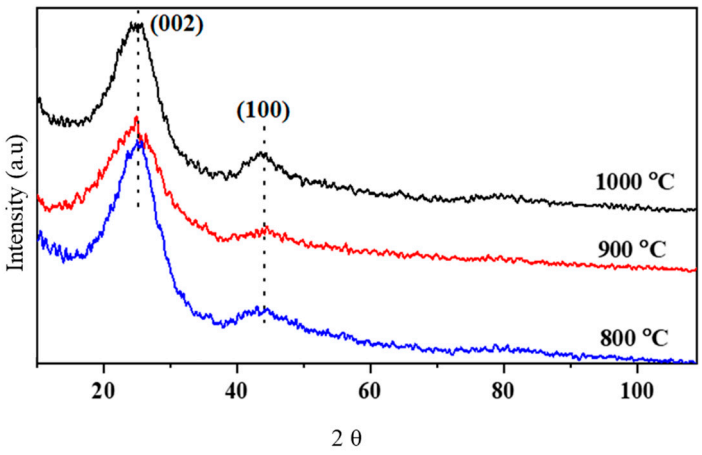

Figure 12. X-ray patterns of the carbon fibers.

Table 3. Parameters of the interlayer distance of carbon nanofibers.

Samples	{002}		{100}	
	2 θ	Distance, D (nm)	2 θ	Distance, D (nm)
CNF 800	24.7251	0.356245	43.6751	0.207083
CNF 900	24.9251	0.357655	43.8751	0.26185
CNF 1000	24.9751	0.35979	44.2251	0.204634

To study the phase composition of the obtained carbon fibers, studies were carried out using Raman spectroscopy (Solver Spectrum, NT-MDT). The Raman light-scattering spectra of the carbon fibers are shown in Figure 13.

In the spectra, the two main broad peaks of 1360 and 1585 cm^{-1} are the bands D and G, corresponding to amorphous carbon. Peak D corresponds to the breathing vibration of the carbon ring C_6, which refers to the hybrid vibrational mode associated with graphene layers. The G-peak is the vibrational mode of sp^2-bound carbon. The ratio of the intensity of band D to the intensity of band G is a measure of the degree of ordering of the carbon structure. Figure 13 shows that the degree of graphitization is calculated with respect to the area of the G-peak compared to the total area of the spectrum in the range from 700 cm^{-1} to 2000 cm^{-1}, and is ~22% at 800 °C and 900 °C and 26.7% for carbonization at 1000 °C.

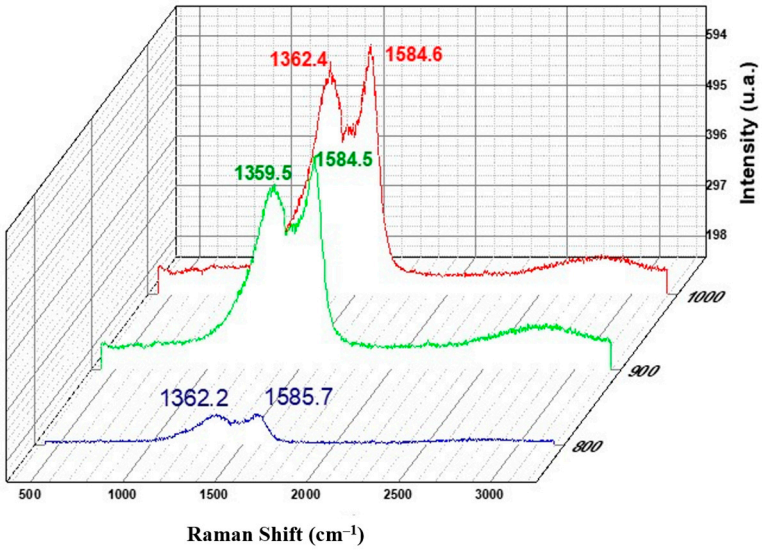

Figure 13. Raman spectra of carbon fibers.

The specific surface area of carbon fiber based on 30/70 lignin/PAN was equal to 549.7 m^2/g. Thus, continuous nanofibers based on lignin/PAN were obtained, and their physicochemical properties were studied using the methods of SEM, optics, EDRS, TGA, Raman spectroscopy. It was revealed that the average value of the fiber diameter distribution was 97 nm.

3.3. Electrochemical Characteristics of Electrodes Based on Nanofibers from Lignin/PAN

To study the electrochemical characteristics, electrodes based on carbon nanofibers made of lignin for supercapacitors and lithium-ion batteries were manufactured, as described in detail in [43]. The specific electrochemical capacitance of the supercapacitor was calculated in accordance with the data of the galvanostatic charge–discharge process of the 30/70 CNF sample at a temperature of 800 °C and a current density of 0.1 A/g, which is equal to 136.4 F/g and, according to cyclic voltammetry, is equal to 92.3 F/g at a scanning speed of 10 Mv/s. Electrodes for lithium-ion batteries were also manufactured. It was found that the carbonization temperature affects the capacity of the material. CNF carbonized at 800 °C has a discharge capacity of 797 mAh/g. This is higher than the value of CNF carbonized at 900 °C, which shows a capacity of 668 mAh/g. Of the three samples, the smallest capacity was demonstrated by the sample carbonized at 1000 °C, which shows 594 mAh/g. CNF-800 demonstrates excellent characteristics and resistance to long service cycles. The obtained data were published earlier in [43].

The operability of the created "button" type CR2032 Li-ion batteries was tested using a simple LED. Experimental laboratory samples of laminar supercapacitors with flat electrodes (pouch cells) were created.

4. Conclusions

The conditions for obtaining lignin from sawdust of elm, pine, and mixed sawdust using the organosolvent method with a higher number of syringyl (S) links compared with guaiacyl (G), which improves the thermal processing of lignin during carbonization, have been optimized. The IR spectra of the obtained lignins indicate the presence of functional groups characteristic of coniferous lignins and the purity of the obtained lignins. Optimal conditions for the production of lignin fibers from mixed wood waste were established, and the influence of technological parameters and concentration of polymer solutions on the structure and morphology of fibers was revealed. It was found that the lignin/PAN ratio of 30:70 allows the synthesis of nanoscale fibers with an average diameter of 97 nm, on the basis of which, by thermal carbonization at 800 °C at a heating rate of 5 °C/min for 60 min in a nitrogen medium, porous carbon nanofibers with a diameter of 47 nm can be obtained.

It was determined that, after carbonization, the carbon content increases, the diameter of the obtained fibers based on lignin/PAN decreases, the alignment of the fiber structure improves, and the tensile strength characteristic improves. The quality of a carbonized fiber depends on the conditions of the carbonization process, such as the temperature, heating rate, gas consumption, and gas medium. Carbon fibers obtained from plant waste are cost-effective and easily accessible.

From a practical point of view, the significance of the work lies, on the one hand, in the development of an environmentally safe method for the disposal of wood waste and lignin from mixed sawdust, and on the other hand, in the development of methods for the production of lignin and carbon nanofibers, which have alternative applications as electrodes in supercapacitors and lithium-ion batteries. The resulting carbon and lignin nanofibers based on wood waste are promising as an electrode material for energy storage systems. Wood waste can form harmful greenhouse gases, including methane. By choosing to recycle wood waste, it is possible to remove wood materials from landfills, reducing their impact on the environment. This contributes to the creation of a more environmentally friendly and sustainable energy landscape.

Author Contributions: Conceptualization, M.N. and B.L.; Methodology, A.B.M.; Investigation, D.D.A. All authors have read and agreed to the published version of the manuscript.

Funding: This research has been funded by the Committee of Science of the Ministry of Science and Higher Education of the Republic of Kazakhstan Grant No. AP14972938 "Development and creation of electrodes for supercapacitors based on nanostructured composite materials", funded by the (2022–2024).

Data Availability Statement: Data are contained within the article.

Acknowledgments: The authors acknowledge the Committee of Science of the Ministry of Science and Higher Education of the Republic of Kazakhstan for their financial support (Grant No. AP14972938).

Conflicts of Interest: The authors declare no conflicts of interest.

References

1. Sharma, S.; Agarwal, S.; Jain, A. Significance of Hydrogen as Economic and Environmentally Friendly Fuel. *Energies* **2021**, *14*, 7389. [CrossRef]
2. Apostolou, D.; Xydis, G. A literature review on hydrogen refueling stations and infrastructure, Current status and future pro-spectus. Renew. *Sustain. Energy Rev.* **2019**, *113*, 109292. [CrossRef]
3. Khan, N.; Kalair, E.; Abas, N.; Kalair, A. Energy transition from molecules to atoms and photons. *Eng. Sci. Technol. Int. J.* **2019**, *22*, 185–214. [CrossRef]
4. Manikandan, S.; Vickram, S.; Sirohi, R.; Subbaiya, R.; Krishnan, R.Y.; Karmegam, N.; Sumathijones, C.; Rajagopal, R.; Chang, S.W.; Ravindran, B.; et al. Critical review of biochemical pathways to transformation of waste and biomass into bioenergy. *Bioresour. Technol.* **2023**, *372*, 128679. [CrossRef] [PubMed]
5. Saleem, M. Possibility of utilizing agriculture biomass as a renewable and sustainable future energy source. *Heliyon* **2022**, *8*, e08905. [CrossRef] [PubMed]
6. Asomaning, J.; Haupt, S.; Chae, M.; Bressler, D.C. Recent developments in microwaveassisted thermal conversion of biomass for fuels and chemicals. *Renew. Sustain. Energy Rev.* **2018**, *92*, 642–657. [CrossRef]
7. Agnihotri, S.; Johnsen, I.A.; Boe, M.S.; Oyaas, K.; Moe, S. Ethanol organosolv pretreatment of softwood (*Picea abies*) and sugarcane bagasse for biofuel and biorefinery applications. *Wood Sci. Technol.* **2015**, *49*, 881–896. [CrossRef]
8. Fabbri, F.; Bischof, S.; Mayr, S.; Gritsch, S.; Jimenez Bartolome, M.; Schwaiger, N.; Guebitz, G.M.; Weiss, R. The Biomodified Lignin Platform: A Review. *Polymers* **2023**, *15*, 1694. [CrossRef]
9. Akhtar, N.; Gupta, K.; Goyal, D.; Goyal, A. Recent Advances in Pretreatment Technologies for Efficient Hydrolysis of Lignocellulosic Biomass. *Environ. Prog. Sustain. Energy* **2016**, *35*, 489–511. [CrossRef]
10. Luck, F.A. A review of industrial catalytic wet air oxidation processes. *Catal. Today* **1996**, *27*, 195–202. [CrossRef]
11. Alvira, P.; Tomas-Pejo, E.; Ballesteros, M.; Negro, M.J. Pretreatment technologies for an efficient bioethanol production process based on enzymatic hydrolysis: A review. *Bioresour. Technol.* **2010**, *101*, 4851–4861. [CrossRef] [PubMed]
12. Sun, Y.; Cheng, J. Hydrolysis of Lignocellulosic Materials for Ethanol Production: A Review. *Bioresour. Technol.* **2002**, *83*, 1–11. [CrossRef] [PubMed]
13. Zhang, K.; Pei, Z.; Wang, D. Organic solvent pretreatment of lignocellulosic biomass for biofuels and biochemicals: A review. *Bioresour. Technol.* **2016**, *199*, 21–33. [CrossRef]

14. Zhao, X.; Liu, D. Fractionating pretreatment of sugarcane bagasse by aqueous formic acid with direct recycle of spent liquor to increase cellulose digestibility-the Formiline process. *Bioresour. Technol.* **2012**, *117*, 25–32. [CrossRef]
15. Long, J.; Xu, Y.; Wang, T.; Yuan, Z.; Shu, R.; Zhang, Q.; Ma, L. Efficient base-catalyzed decomposition and in situ hydrogenolysis process for lignin depolymerization and char elimination. *Appl. Energy* **2015**, *141*, 70–79. [CrossRef]
16. Fodil, C.; Trache, D.; Brosse, N.; Benaliouche, F.; Tarchoun, A.F. Comparison of the physicochemical properties and thermal stability of organosolv and kraft lignins from hardwood and softwood biomass for their potential valorization. *Waste Biomass Valorization* **2020**, *11*, 6541–6553. [CrossRef]
17. Nasim, R.; Mohini, S. Thermal and Physiochemical Characterization of Lignin Extracted from Wheat Straw by Organosolv Process. *J. Polym. Environ.* **2018**, *26*, 3109–3116.
18. Lallave, M.; Bedia, J.; Ruiz-Rosas, R.; Rodríguez-Mirasol, J.; Cordero, T.; Otero, J.C.; Marquez, M.; Barrero, A.; Loscerales, I.G. Filled and hollow carbon nanofibers by coaxial electrospinning of alcell lignin without binder polymers. *Adv. Mater.* **2007**, *19*, 4292–4296. [CrossRef]
19. Sun, J.; Jiang, H.R.; Wu, M.C.; Fan, X.Z.; Chao, C.Y.H.; Zhao, T.S. A novel electrode formed with electrospun nano- and micro-scale carbon fibers for aqueous redox flow batteries. *J. Power Sources* **2020**, *470*, 228441. [CrossRef]
20. Ali, W.; Shabani, V.; Linke, M.; Sayin, S.; Gebert, B.; Altinpinar, S.; Hildebrandt, M.; Gutmann, J.S.; Mayer-Gall, T. Electrical conductivity of silver nanoparticle doped carbon nanofibres measured by CS-AFM. *RSC Adv.* **2019**, *9*, 4553–4562. [CrossRef]
21. Su, C.; Tong, Y.; Zhang, M.; Zhang, Y.; Shao, C. TiO_2nanoparticles immobilized on polyacrylonitrile nanofibers mats: A flexible and recyclable photocatalyst for phenol degradation. *RSC Adv.* **2013**, *3*, 7503–7512. [CrossRef]
22. Khayyam, H.; Jazar, R.N.; Nunna, S.; Golkarnarenji, G.; Badii, K.; Fakhrhoseini, S.M.; Kumar, S.; Naebe, M. PAN precursor fab-rication, applications and thermal stabilization process in carbon fiber production: Experimental and mathematical modelling. *Prog. Mater. Sci.* **2020**, *107*, 100575. [CrossRef]
23. Ramdayal, Y.; Omid, Z.; Sobhan, F.; Hossein, A.N.; Alper, K.; Patrick, B.; Minoo, N. Lignin derived carbon fiber and nanofiber: Manufacturing and applications. *Compos. Part B Eng.* **2023**, *255*, 110613.
24. Ruiz-Rosas, R.; Bedia, J.; Lallave, M.; Loscertales, I.G.; Barrero, A.; Rodríguez-Mirasol, J.; Cordero, T. The production of submicron diameter carbon fibers by the electrospinning of lignin. *Carbon* **2010**, *48*, 696–705. [CrossRef]
25. Wang, S.; Bai, J.; Innocent, M.T.; Wang, Q.; Xiang, H.; Tang, J.; Zhu, M. Lignin-based carbon fibers: Formation, modification and potential applications. *Green Energy Environ.* **2022**, *7*, 578–605. [CrossRef]
26. Jan, J.; Yu, B.-J.; Shi, Z.-Q.; Wang, C.-Y.; Chong, C.-B. Lignin-based electrospun carbon nanofibrous webs as free-standing and binder-free electrodes for sodium ion batteries. *J. Power Sources* **2014**, *272*, 800–807. [CrossRef]
27. Peuvot, K.; Hosseinaei, O.; Tomani, P.; Zenkert, D.; Lindbergh, G. Lignin Based Electrospun Carbon Fiber Anode for Sodium Ion Batteries. *J. Electrochem. Soc.* **2019**, *166*, A1984–A1990. [CrossRef]
28. García-Mateos, F.J.; Ruiz-Rosas, R.; María Rosas, J.; Moralloń, E.; Cazorla-Amorós, D.; Rodríguez-Mirasol, J.; Cordero, T. Activation of Electrospun Lignin-Based Carbon Fibers and Their Performance as Self-Standing Supercapacitor Electrodes. *Sep. Purif. Technol.* **2020**, *241*, 116724. [CrossRef]
29. Zhang, W.; Yang, P.; Luo, M.; Wang, X.; Zhang, T.; Chen, W.; Zhou, X. Fast Oxygen, Nitrogen Co-Functionalization on Elec-trospun Lignin-Based Carbon Nanofibers Membrane via Air Plasma for Energy Storage Application. *Int. J. Biol. Macromol.* **2020**, *143*, 434–442. [CrossRef]
30. Jeong, J.H.; Lee, Y.H.; Kim, B.H. Relationship between Microstructure and Electrochemical Properties of 2lignin-Derived Carbon Nanofibers Prepared by Thermal Treatment. *Synth. Met.* **2020**, *260*, 116287. [CrossRef]
31. Herou, S.; Crespo, M.; Titirici, M. Investigating the Effects of Activating Agent Morphology on the Porosity and Related Capacitance of Nanoporous Carbons. *CrystEngComm* **2020**, *22*, 1560–1567. [CrossRef]
32. Boeriu, C.G.; Bravo, D.; Gosselink, R.J.; van Dam, J.E. Characterisation of structure-dependent functional properties of lignin with infrared spectroscopy. *Ind. Crops Prod.* **2004**, *20*, 205–218. [CrossRef]
33. Tejado, A.; Pena, C.; Labidi, J.; Echeverria, J.M.; Mondragon, I. Physico-chemical characterization of lignins from different sources for use in phenol-formaldehyde resin synthesis. *Bioresour Technol.* **2007**, *98*, 1655–1663. [CrossRef] [PubMed]
34. Elshafie, M.; Taha, M.G.; Elhamamsy, S.M.; Moustafa, Y.; Elazab, W.I.M. Thermal analysis of the prepared lignin/graphene oxide/polyurethane composite/Egyptian. *J. Pet.* **2020**, *29*, 8.
35. Lundquist, K. NMR studies of lignins. Investigation of spruce lignin by 1H NMR spectroscopy. *Acta Chem. Scand.* **1980**, *34*, 21–26. [CrossRef]
36. Saliba, E.D.; Rodriguez, N.M.; de Morais, A.; Piló-Veloso, D. Ligninas: Métodos de obtenção e caracterização química. *Ciência Rural.* **2001**, *31*, 917–928. [CrossRef]
37. Lundquist, K. Proton (1H) NMR spectroscopy. In *Methods in Lignin Chemistry*; Springer: Berlin, Germany, 1992; pp. 242–249.
38. Papkov, D.; Zou, Y.; Andalib, M.N.; Goponenko, A.; Cheng, S.Z.D.; Dzenis, Y.A. Simultaneously strong and tough ultrafine continuous nanofibers. *ACS Nano* **2013**, *7*, 3324–3331. [CrossRef]
39. Naraghi, M.; Arshad, S.N.; Chasiotis, I. Molecular orientation and mechanical property size effects in electrospun polyacrylonitrile nanofibers. *Polymer* **2011**, *52*, 1612–1618. [CrossRef]
40. Yarin, A.L.; Koombhongse, S.; Reneker, D.H. Bending instability in electrospinning of nanofibers. *J. Appl. Phys.* **2001**, *5*, 89. [CrossRef]

41. Ji, L.; Zhang, X. Manganese oxide nanoparticle-loaded porous carbon nanofibers as anode materials for high-performance lithium-ion batteries. *Electrochem. Commun.* **2009**, *11*, 795–798. [CrossRef]
42. Peng, Y.T.; Lo, C.T. Effect of Microstructure and Morphology of Electrospun Ultra-Small Carbon Nanofibers on Anode Performances for Lithium Ion Batteries. *J. Electrochem. Soc.* **2015**, *162*, 1085–1093. [CrossRef]
43. Nazhipkyzy, M.; Maltay, A.B.; Askaruly, K.; Assylkhanova, D.D.; Seitkazinova, A.R.; Mansurov, Z.A. Biomass-Derived Porous Carbon Materials for Li-Ion Battery. *Nanomaterials* **2022**, *12*, 3710. [CrossRef] [PubMed]